Correlation of Transverse and Rotational Diffusion Coefficient: A Probe of Chemical Composition in Hydrocarbon Oils

Albina R. Mutina

Kazan State University, Kremlevskaya Str., 18, 420008 Kazan, Russia

Martin D. Hürlimann*

Schlumberger-Doll Research, One Hampshire Street, Cambridge, Massachusetts 02139

Received: October 23, 2007; In Final Form: January 28, 2008

Measurements of relaxation time and diffusion coefficient by nuclear magnetic resonance are well-established techniques to study molecular motions in fluids. Diffusion measurements sense the translational diffusion coefficients of the molecules, whereas relaxation times measured at low magnetic fields probe predominantly the rotational diffusion of the molecules. Many complex fluids are composed of a mixture of molecules with a wide distribution of sizes and chemical properties. This results in correspondingly wide distributions of measured diffusion coefficients and relaxation times. To first order, these distributions are determined by the distribution of molecular sizes. Here we show that additional information can be obtained on the chemical composition by measuring two-dimensional diffusion−relaxation distribution functions, a quantity that depends also on the shape and chemical interactions of molecules. We illustrate this with experimental results of diffusion−relaxation distribution functions on a series of hydrocarbon mixtures. For oils without significant amounts of asphaltenes, the diffusion−relaxation distribution functions follow a power-law behavior with an exponent that depends on the relative abundance of saturates and aromatics. Oils with asphaltene deviate from this trend, as asphaltene molecules act as relaxation contrast agent for other molecules without affecting their diffusion coefficient significantly. In waxy oils below the wax appearance temperature a gel forms. This is reflected in the measured diffusion−relaxation distribution functions, where the restrictions due to the gel network reduce the diffusion coefficients without affecting the relaxation rates significantly.

I. Introduction

Many naturally occurring fluids are complex mixtures of molecules with a wide range of size and chemical properties. For the understanding and prediction of fluid properties such as viscosity and the onset temperature of gelling, waxing or other phase transitions, it is essential to have an accurate knowledge of the distribution of molecular sizes and the chemical composition. Techniques to determine the distribution of molecular sizes include gas chromatography,[1] mass spectroscopy[2] and nuclear magnetic resonance (NMR) relaxation and diffusion measurements.[3,4] Information on chemical composition can be obtained by standard chemical analysis[5] or spectroscopy, such as NMR[6] or optical spectroscopies.

In this paper, we discuss a new approach to obtain chemical information based on low field NMR measurements, in particular from the measurement of two-dimensional distribution functions between diffusion and relaxation. We concentrate on distribution functions between translational diffusion and transverse relaxation,[7] and on distribution functions between longitudinal and transverse relaxation.[8] At low fields, the diffusion−relaxation distribution functions are related to the distribution functions between translational and rotational diffusion coefficient, a quantity that depends on the shapes of the molecules and their interactions. Distribution functions between longitudinal and transverse relaxation times are particularly sensitive to motion below the Larmor frequency and are therefore able to detect the presence of large molecules and aggregates.

The translational diffusion properties of molecules in simple fluids is mainly controlled by the molecular size and to a lesser degree by their shapes. Proton NMR relaxation in simple fluids is typically dominated by dipolar interactions, modulated by the local motions of the molecules and has been studied extensively.[9,10] For small molecules with large rotational diffusion coefficients, the rapid molecular tumbling averages out the dipolar interactions of adjacent spins to a high degree. This results in long relaxation times. For larger molecules, the rotational diffusion coefficients decrease and the observed transverse relaxation times T_2 decrease accordingly. As long as the tumbling frequency is high compared to the Larmor frequency, the system is in the fast motion regime and the longitudinal and transverse relaxation times, T_1 and T_2, respectively, are equal. When the fluid contains large molecules or aggregates, some of the tumbling motions are slower than the Larmor frequency and the two relaxation times T_1 and T_2 differ. In such cases, both the overall molecular reorientation and the internal molecular motion have to be considered.[11]

In complex fluids of interest here, it is necessary to use distributions to describe both the relaxation and diffusion properties of the sample. We denote these distribution functions by $f(T_2)$ and $f(D)$, respectively. To first order, we expect that the range of relaxation times and diffusion coefficients is a measure of the range of molecular sizes in the fluid. As an illustration, Freed et al.[3,4] found that for mixtures of alkanes, both the measured diffusion coefficients D and transverse relaxation time T_2 show a power-law dependence on chain length

10.1021/jp710254d CCC: $40.75
Published on Web 03/12/2008

TABLE 1: Properties of the 12 Samples Used in This Study[a]

sample	saturates		aromatics		resin		asphaltenes		density	wax	η (cP])
#1	96.2	85.1	3.7	8.2	0.1	5.8	0.0	0.13	0.797	20.0	11.5
#2	67.1	73.9	24.9	13.6	7.9	10.5	0.0	0.03	0.845	11.5	9.4
#3	59.4	72.2	26.9	15.8	13.6	10.6	0.1	0.05	0.849	11.9	4.0
#4	52.6	60.6	31.3	17.7	15.2	22.1	0.9	0.20	0.859	8.4	5.8
#5	61.3	60.5	34.5	23.0	4.2	11.0	0.0	0.04	0.881	9.7	24.1
#6	51.2	70.0	38.7	10.2	10.0	17.0	0.1	0.02	0.925	2.7	31.3
#7	50.1	65.7	38.0	16.8	11.7	11.2	0.2	0.13	0.921	2.8	25.5
#8		72.8		18.4		5.5		0.01			
#9	37.9	39.9	32.4	22.2	18.3	26.1	12.9	8.16	0.916	7.1	72.7
#10	52.1	54.7	27.2	17.3	16.1	25.3	4.9	2.71	0.883	5.9	23.2
#11	47.0	49.7	27.3	18.0	18.7	27.3	7.6	2.4	0.886	8.6	30.2
#12	45.9	53.5	33.9	18.8	17.3	26.9	3.0	1.17	0.874	8.4	35.5

[a] The results of the SARA analysis (in weight percent) performed by Intertek Westport Technology Center, Houston, are shown in the left columns, whereas those by Oilphase-DBR, Edmonton, Canada, are displayed on the right. Also shown are the densities at 25 °C (in g/cm^3), the wax concentration (sum of all *n*-alkanes, in weight percent), and the viscosity.

over a surprisingly large range. In such systems, it is then possible to relate the distribution of measured relaxation times directly to the distribution of chain length of the alkane molecules. Diffusion and relaxation distribution functions are directly related to each other.

In the more general case when the components of the fluids not only are of different size but also have different shapes, a more complex response is anticipated. The two-dimensional diffusion−relaxation distribution function $f(D,T_2)$ probes the relationship between translational and rotational diffusion coefficient for each component. The shape of this distribution function is then a fingerprint of the fluid and reflects the composition of the fluid.

We have tested this approach by measuring systematically distribution functions $f(D,T_2)$ and $f(T_1,T_2)$ for a dozen hydrocarbon samples with a range of viscosities and chemical composition.[12,13] These oils consist of a mixture of components, including chainlike molecules such as alkanes, aromatic molecules that contain ringlike components, and larger, polar asphaltene molecules that have a high tendency to aggregate.[14]

A key advantage of these NMR based measurements is that they can be performed noninvasively, even when the fluid is contained in a nontransparent holder or fills the pore space of porous media.[15] In addition, the requirement on the strength and homogeneity of the magnetic field is much less stringent than for conventional NMR measurements. Magnet systems based on permanent magnets and ex-situ configurations are well suited for this purpose.

The paper is organized as follows: In section II, the samples and their compositions are discussed. Details of the experimental NMR techniques and analysis are presented in section III. Results of the measured distribution functions of $f(D,T_2)$ and $f(T_1,T_2)$ and their temperature dependences are given in section IV. The results are analyzed and discussed in section V. The conclusions are presented in section VI.

II. Samples

We studied 12 hydrocarbon samples, collected from different oil fields, that cover a range of chemical composition and viscosity. The samples are stock tank oils that have been stored at room temperature and ambient pressure for a number of years and lost the volatile components. The oils were deoxygenated with a freeze-vacuum-thaw technique[16] to remove oxygen (that is paramagnetic) and eliminate its effect on the NMR relaxation times. The samples were then sealed in cylindrical glass ampoules of 25 mL volume.

A standard method to characterize the overall composition is to perform a so-called SARA analysis that divides the oils into four fractions with different polarities and solubilities.[12] The four components are referred to as saturates, aromatics, resins, and asphaltenes. Asphaltenes[12,14] are by definition insoluble in *n*-heptane and are first precipitated from the oil. After filtering out the asphaltenes and removing the *n*-heptane, the remaining sample is referred to as maltene. It is separated into the three remaining fraction by liquid chromatography.[17] Results of the SARA analysis for our oils, performed independently in two different laboratories, are given in Table 1. It is well-known that results of the SARA analysis depend somewhat on the details of the laboratory procedure used in its implementation.[18] Although the reproducibility for a given procedure is typically 1% or better, differences obtained with different procedures are often significantly larger, as is evident in Table 1. As an example, the procedure by Oilphase-DBR to quantify the asphaltene components includes extra steps to remove any trapped saturates in the precipitate.[19] It is therefore not surprising that the asphaltene concentrations reported by Intertek Westport are systematically higher than those reported by Oilphase-DBR.

In addition to the measurements shown in Table 1, high-temperature gas chromatography measurements were performed on the maltenes by Oilphase-DBR, Edmonton, Alberta, Canada. The gas chromatography results are shown in Figure 1. In each panel, the upper curve shows the concentration of molecules with a certain carbon number N_i, whereas the lower curve shows the concentration of *n*-alkanes. This separation is possible because the *n*-alkanes have well-defined retention times and appear as sharp peaks that can be separated from the rest of the signal.

On the basis of the results in Table 1 and Figure 1, we group the oils into three classes of oil. These groups have been indicated by horizontal separators in Table 1 and have been placed in different columns in Figure 1. We call the three classes by their main features: class 1, saturate rich oils; class 2, aromatic rich oils; class 3, oils with asphaltene.

Oils in class 1 and 2 have no significant amounts of asphaltene. Oils with a least 1% of asphaltenes form class 3. These oils have also relatively high levels of resin. The difference between oils in class 1 and class 2 is most apparent from the results of the gas chromatography: oils in class 2 have abnormally low levels of *n*-alkanes. In addition, the chain length distribution for the organics is not decaying monotonically with chain length in these oils. The SARA results also show that these oils tend to have high levels of aromatics and high

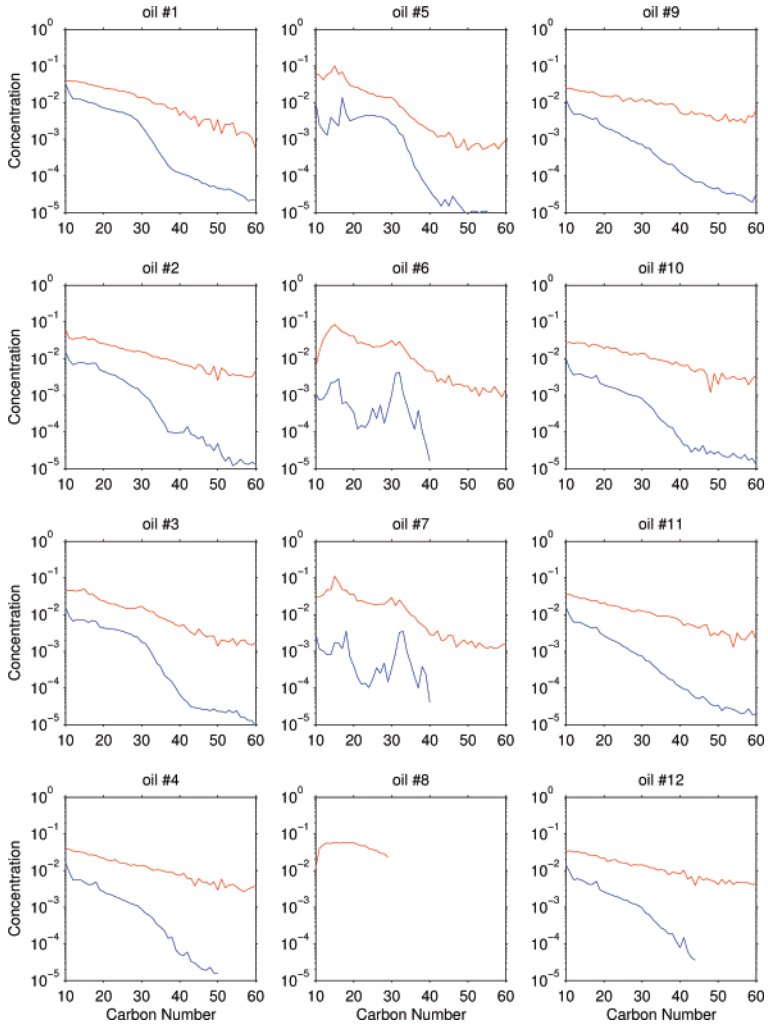

Figure 1. Gas chromatography data for the maltenes of the 12 samples. The upper curves show the total organics content, whereas the lower curves show only the *n*-alkanes. For sample 8, the information of *n*-alkanes is not available.

densities. Oils with significant biodegradation and no asphaltene will fall into class 2.

III. Experimental Techniques

NMR measurements of low-field relaxation and diffusion were performed in the fringe field outside of a horizontal bore 2 T magnet at a Larmor frequency 5.03 MHz and associated field gradient of $g = 54.4$ G/cm, unless otherwise noted. The techniques used to measure the two-dimensional distribution functions $f(D,T_2)$ and $f(T_1,T_2)$ are described in detail in refs 7 and 20. Here D is the diffusion coefficient, and T_2 and T_1 are the transverse and longitudinal relaxation times, respectively. The durations of the 180° and 90° pulses were typically $t_{180} = 22\ \mu s$ and $t_{90} = 12\ \mu s$, respectively.

We used the pulse sequence (a) in Figure 2 to measure the diffusion$-T_2$ distribution functions $f(D,T_2)$ of the majority of samples.[7] The sequence consists of an initial stimulated echo sequence, followed by a long train of 180° refocusing pulses. The time between the first and second 90° pulse (which is equal to the time between the third 90° pulse and the stimulated echo) was systematically changed in the range of 200 μs to 16 ms to obtain diffusion sensitivity over the full range of interest. The time between the first 90° pulse and the stimulated echo was kept constant at $T_d = 40$ ms. We acquired 8000 echoes with an echo spacing $t_E = 298\ \mu s$. The initial data processing followed the procedure outlined in[7] and included filtering of the echoes and correction of the initial transient effect due to off-resonance effects. The echo amplitudes are then related to the distribution function $f(D,T_2)$ for spins surviving at time T_d by

$$A(t,\delta) = \int\int \mathrm{d}D\ \mathrm{d}T_2\ f(D,T_2) \exp\left\{-\gamma^2 g^2 \delta^2 D\left(T_d - \frac{4\delta}{3}\right)\right\} \exp\left\{-\frac{t}{T_2}\right\} \quad (1)$$

Here γ is the gyromagnetic ratio, g is the applied magnetic field gradient, and t is the time after the stimulated echo. The distribution function $f(D,T_2)$ is extracted from the measured amplitudes using the algorithm for inverse fast Laplace transformation described in ref 21. The regularization parameter α in this optimization procedure was typically chosen to be $\alpha = 10$.

For measurements at the higher temperatures, convection effects interfered with the diffusion measurements. This problem can be avoided by using sequence (b), where the initial echo spacings $t_{E,1}$ are systematically increased to encode diffusion. As was first pointed out by Carr and Purcell,[22] the second echo is compensated for flow effects. As a consequence, the echoes collected with sequence (b) are not affected by convection effects during the encoding time.

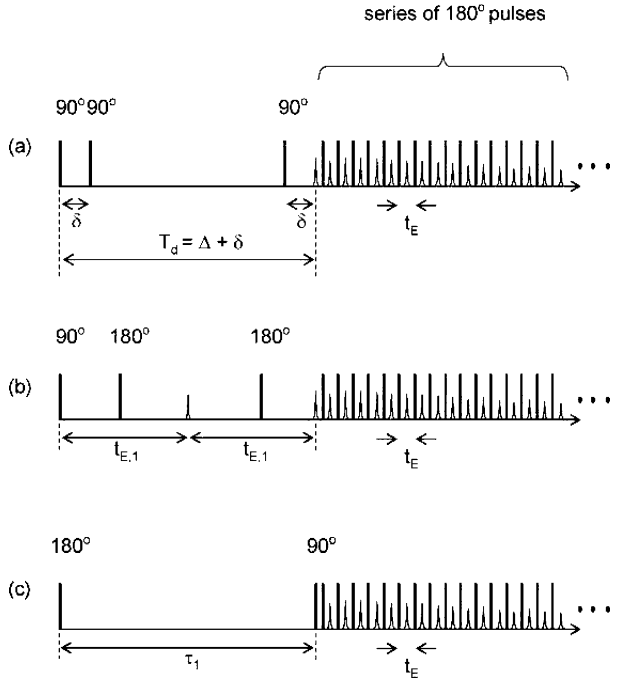

Figure 2. Pulse sequence to measure 2d distribution functions in the presence of a constant gradient. The first two sequences are examples to measure $f(D,T_2)$, consisting of a diffusion encoding subunit, followed by the CPMG sequence. In (a) the diffusion editing is based on a stimulated echo, whereas in (b) it is based on the second direct echo with increased echo spacing. The bottom sequence in (c) was used to measure a $f(T_1,T_2)$. The T_1 editing is achieved by an inversion−recovery sequence.

TABLE 2: Exponents ζ for Class I and Class II Oils Extracted from Experimental Data Shown in Figure 3

sample	exponent ζ	sample	exponent ζ
#1	0.84	#5	0.55
#2	0.71	#6	0.45
#3	0.69	#7	0.53
#4	0.82	#8	0.54

T_1-T_2 distribution functions were measured with the pulse sequence of Figure 2 (c). It is based on the inversion−recovery sequence, $180°-\tau_1-90°$, followed again by a long train of refocusing pulses. The recovery time τ_1 was changed logarithmically in the range of 1 ms to 10 s in 30 steps. As for the $D-T_2$ measurements, we acquired 8000 echoes with an echo spacing of 298 μs. As described ref 7, we first filtered the echoes, subtracted the fully recovered signal, and corrected the transient effect of the first few echoes caused by off-resonance effects. The resulting amplitudes for the T_1-T_2 experiment are then given by

$$A(t,\tau_1) = \int\int \mathrm{d}T_1\, \mathrm{d}T_2\, f(T_1,T_2) \exp\left\{-\frac{\tau_1}{T_1}\right\} \exp\left\{-\frac{t}{T_2}\right\} \quad (2)$$

To measure small diffusion coefficients associated with the heavier oils, relatively large field gradients are required. It is convenient to use static gradients to avoid eddy current effects.[23] However, for samples with higher diffusion coefficients and long relaxation times, the presence of a static gradient during the CPMG sequence contributes an extra decay rate to the observed signal due to diffusion that is of the order of $\gamma^2 g^2 D t_E^2/12$. In the present results, this effect is only noticeable for relaxation times longer than 1 s.

Measurements were performed at temperatures between 5 and 57 °C. The temperature of the samples were controlled within 0.1 °C.

IV. Results

A. Diffusion$-T_2$ Distribution Function. Figure 3 gives an overview of the measured distribution functions $f(D,T_2)$ for the 12 oils at $T = 30$ °C. The distribution functions typically extend over a decade in diffusion coefficients and relaxation times, reflecting the wide distribution of chain lengths in the oils. As a reference, we have included in the plots of $f(D,T_2)$ the "alkane line" $D = \beta T_2$, where $\beta = 5 \times 10^{-10}$ m^2/s^2. This line follows the correlation between the mean diffusion coefficient and mean T_1 of pure alkanes reported in ref 24.

We can immediately draw two conclusions. First, the diffusion$-T_2$ distribution function is a distinct fingerprint of an oil. Second, the measured distribution function $f(D,T_2)$ for oils within a given class share general properties: Oils in class I display contributions that are approximately along the alkane line. The contributions for oils in class II are also generally close to the alkane line, but with a slope that is significantly smaller than for class I oils. Finally, oils with asphaltene (class III) have contributions that are clearly above the alkane line.

Oils of class I and II show a strong correlation between the measured diffusion coefficient and transverse relaxation time. For these oils, the center of the contributions of $f(D,T_2)$ is close to the alkane reference line and the relationship between the diffusion coefficient of a component, D_i, and the corresponding relaxation time, $T_{2,i}$, can be well approximated by a power law:

$$\frac{D_i}{\langle D\rangle} = \left(\frac{T_{2,i}}{\langle T_2\rangle}\right)^{\zeta} \quad (3)$$

Oils in class I can be distinguished from oils in class II by the exponents ζ. The values ζ extracted from the measured distribution functions, using a least-squared optimization, are listed in Table 2. The exponents for oils with high fraction of saturates (class I) are clustered between 0.7 and 0.85, whereas those for class II oils are clustered around 0.5.

Oils with a significant fraction of asphaltene (class III) are also easily identified from the distribution function $f(D,T_2)$. For all such oils, the main contributions in $f(D,T_2)$ lie systematically above the alkane line. In Figure 4, we display the centers of mass $(\langle D\rangle,\langle T_2\rangle)$ extracted from the diffusion−relaxation time distribution functions shown in Figure 3. Here the averages are defined by $\log\langle D\rangle = \langle\log(D_i)\rangle$ and $\log\langle T_2\rangle = \langle\log(T_{2,i})\rangle$. For oils without asphaltene, the averages cluster around the alkane line, whereas for oils with asphaltene, the averages clearly lie above this line. At lower temperatures, a number of oils show wax precipitation. As discussed in section IV.C.1, this leads to a deviation of the center of mass below the alkane line.

B. T_1-T_2 Distribution Function. The results for the T_1-T_2 distribution functions $f(T_1,T_2)$ are shown in Figure 5 for $T = 30$ °C. It is remarkable that for a given oil the ratios T_1/T_2 for the individual components are nearly constant; i.e., the contributions of $f(T_1,T_2)$ are confined to a line along or parallel to the reference line $T_1 = T_2$. Close inspection shows that for oils with relaxation times longer than 1 s, the distributions slightly bend away from a constant T_1/T_2 ratio at the longest relaxation times. This is caused by diffusion effects in the static gradient[26] that shorten the measured transverse relaxation times. Comparing the response of different oils, we find that the T_1/T_2 ratio is sample specific. The ratio is close to 1 for oils without

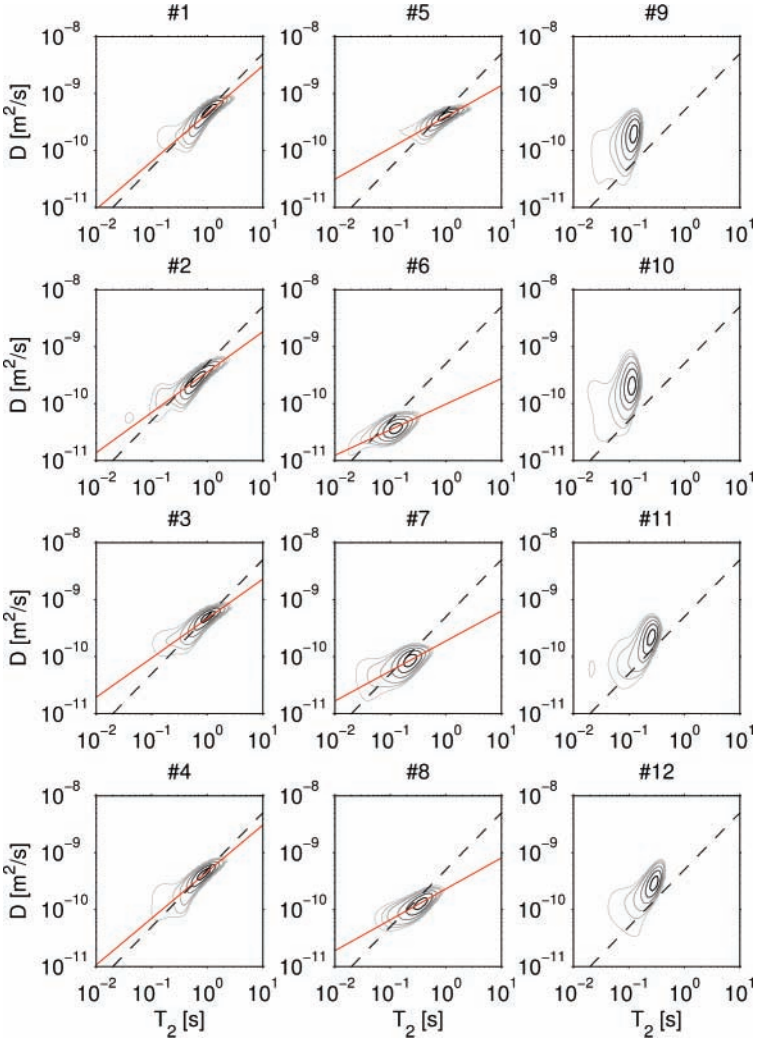

Figure 3. Measured distribution functions between diffusion and transverse relaxation time, $f(D,T_2)$, for the 12 deoxygenated oils at $T = 30$ °C. In each panel, the dashed line is the "alkane line" that indicates the correlation between the mean diffusion coefficient and mean T_1 of pure alkanes reported in ref 24. The red solid lines are fits to the power-law behavior of eq 3. Contour lines are drawn at 10%, 20%, 30%, 50%, 70% and 90% of the maximum values of each distribution function. The oils are arranged in columns according to the composition class discussed in section II.

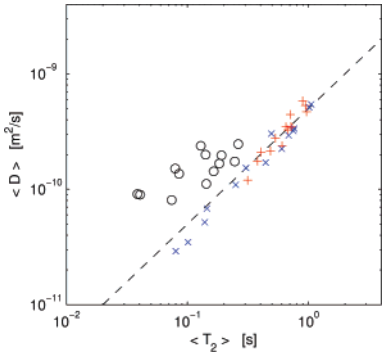

Figure 4. Center of mass of the measured distribution functions $f(D,T_2)$ for all oils. The plot contains results from measurements at temperatures between 10 and 50 °C. Results for oils of different classes are identified by different symbols: (+) class I oils; (×) class II oils; (○) class III oils. The dashed line shows the alkane line, i.e., the correlation between the mean diffusion coefficient and mean T_1 of pure alkanes.[24] Oils with asphaltene (class III oils) all appear above the alkane line and are easily identified in this plot.

asphaltene (class I and II), and significantly larger than 1 for oils with asphaltene (class III oils).

The T_1/T_2 ratio therefore provides an alternative method to infer whether an oil has significant amounts of asphaltene. In Figure 6, we plot the centers of mass of the T_1-T_2 distribution functions for all the oils. Oils with asphaltene (class III) clearly stand out and are easily identified.

C. Temperature Dependence. The temperature dependence of the diffusion$-T_2$ distribution functions for three representative oils are shown in Figure 7. The three oils (#4, #7, and #10) are members of the three different classes and stay single-phase over the whole temperature range studied. The figure shows distributions measured at three different temperatures, 10 °C (blue), 30 °C (black), and 50 °C (red).

As the temperature is increased, the oil viscosity decreases and as a consequence, the diffusion coefficients and relaxation times increase, as expected. Note that for each oil, the shape of the distribution function is to first-order unaffected by temperature. This implies that for oils in class I and II the relationship of eq 3 is preserved, with an exponent ζ that is to first order independent of temperature.

When the temperature is changed, the observed overall shift of the diffusion−relaxation time distribution function is predominantly parallel to the alkane line for all three oils. Within the experimental uncertainties, the relative shift in the measured

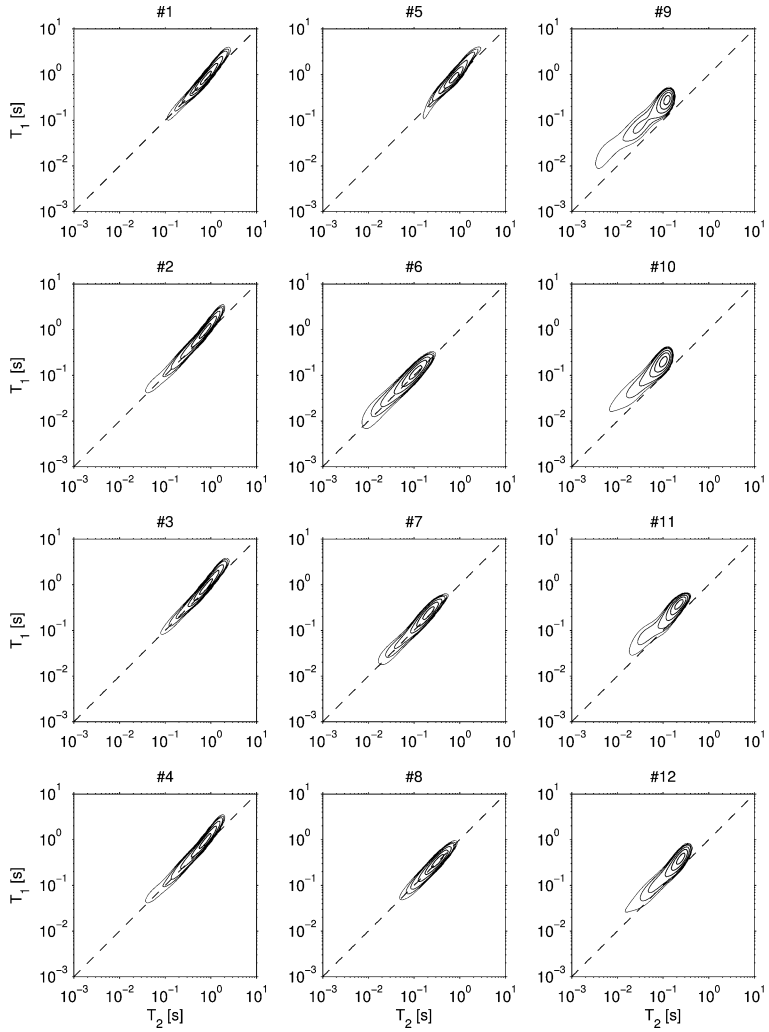

Figure 5. Measured distribution functions between longitudinal and transverse relaxation time, $f(T_1,T_2)$ for the 12 oils at $T = 30$ °C. The dashed lines indicate $T_1 = T_2$. The oils are arranged in columns according to the composition class, identically to Figure 3. Oils with significant amounts of asphaltene, displayed in the third column, show consistently T_1/T_2 ratios larger than 1.

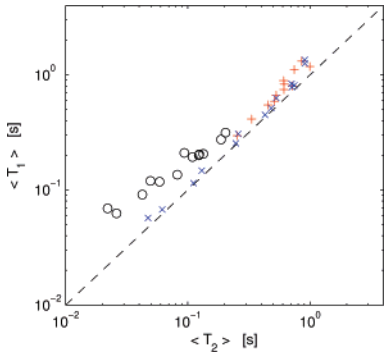

Figure 6. Center of mass of the measured distribution functions $f(T_1,T_2)$ for all oils. The plot contains results from measurements at temperatures between 10 and 50 °C. Results for oils of different classes are identified by different symbols: (+) class I oils; (×) class II oils; (○) class III oils. The dashed line indicates $T_1 = T_2$. Oils with asphaltene (class III oils) are easily identified in this plot.

diffusion coefficients equals that in the relaxation times:

$$\frac{\langle D\rangle(T)}{\langle D\rangle(T_0)} \cong \frac{\langle T_2\rangle(T)}{\langle T_2\rangle(T_0)} \tag{4}$$

This behavior is consistent with the temperature dependence of the average relaxation time and diffusion coefficients of oils reported by Straley in ref 27. This indicates that over the temperature range studied, the temperature dependence of the diffusion coefficient and relaxation time is dominated by the same underlying quantity, i.e., the internal viscosity.[3,4]

The results presented in Figure 7 demonstrate that the features in $f(D,T_2)$ used to infer the general composition are to first order independent of temperature. The distance of the center of mass from the alkane line stays constant, as the slope of the dominant feature. Therefore, the correspondence between general features of composition and features in the distribution function holds over the full temperature range.

1. Waxy Oils. Crude oils with a significant fraction of long-chain *n*-paraffins are generally classified as waxy oils[12] and have a high wax appearance temperature. When such crude oils are cooled, the long-chain molecules tend to crystallize below the wax appearance temperature and form a gel.[28,29] The formation of such organogels drastically increases the viscosity and can lead to numerous problems during production, transportation or processing of crude oil.

Among our samples, Table 1 indicates that oil #1 has the highest wax content with 20%. As the temperature is reduced below 20 °C, this oil becomes cloudy and wax crystals appear. The viscosity increases drastically and the sample appears to be solidlike. This waxing behavior is reflected in the diffusion−

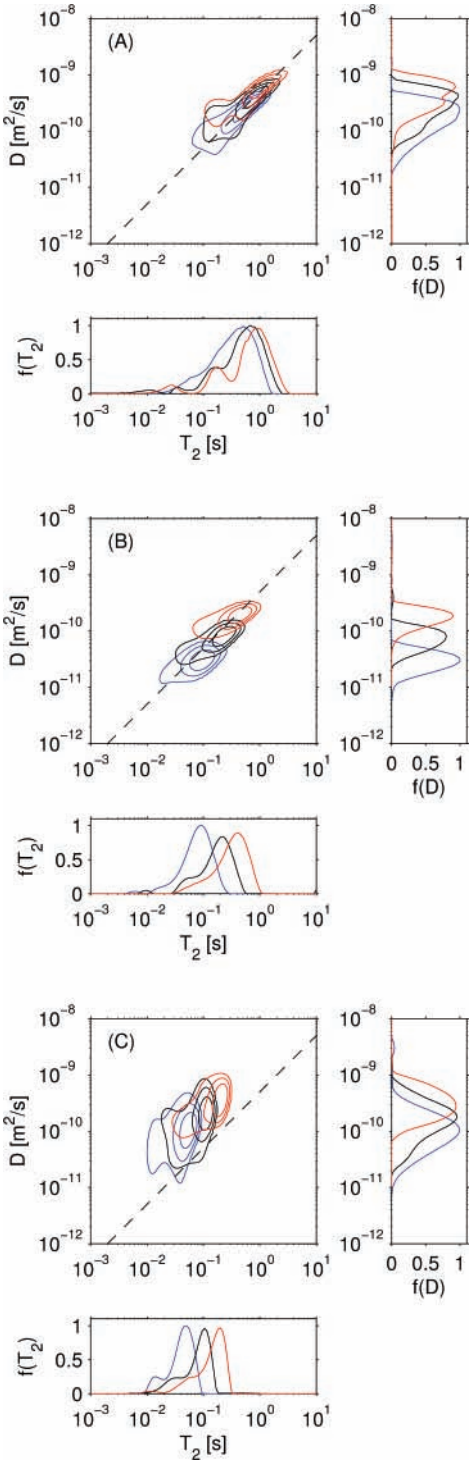

Figure 7. Diffusion−T_2 relaxation distribution functions for oils representing the different classes at three different temperatures, 10, 30 and 50 °C, shown as blue, black, and red contours, respectively: (A) saturate rich oil, #4; (B) aromatic rich oil, #7; (C) an oil with significant amounts of asphaltene, #10.

T_2 measurements, as shown in Figure 8. As the temperature is lowered, the main contribution in $f(D,T_2)$ moves below the alkane line. Even though the overall viscosity of the sample increases drastically and the oil stops flowing, the relaxation times do not decrease greatly and the diffusion coefficients decrease by less than an order of magnitude. The experiments therefore indicate that the motion of the detected spins are still fluidlike.

These observations are consistent with the presence of a gel that consists of a cross-linked network and a liquid component.

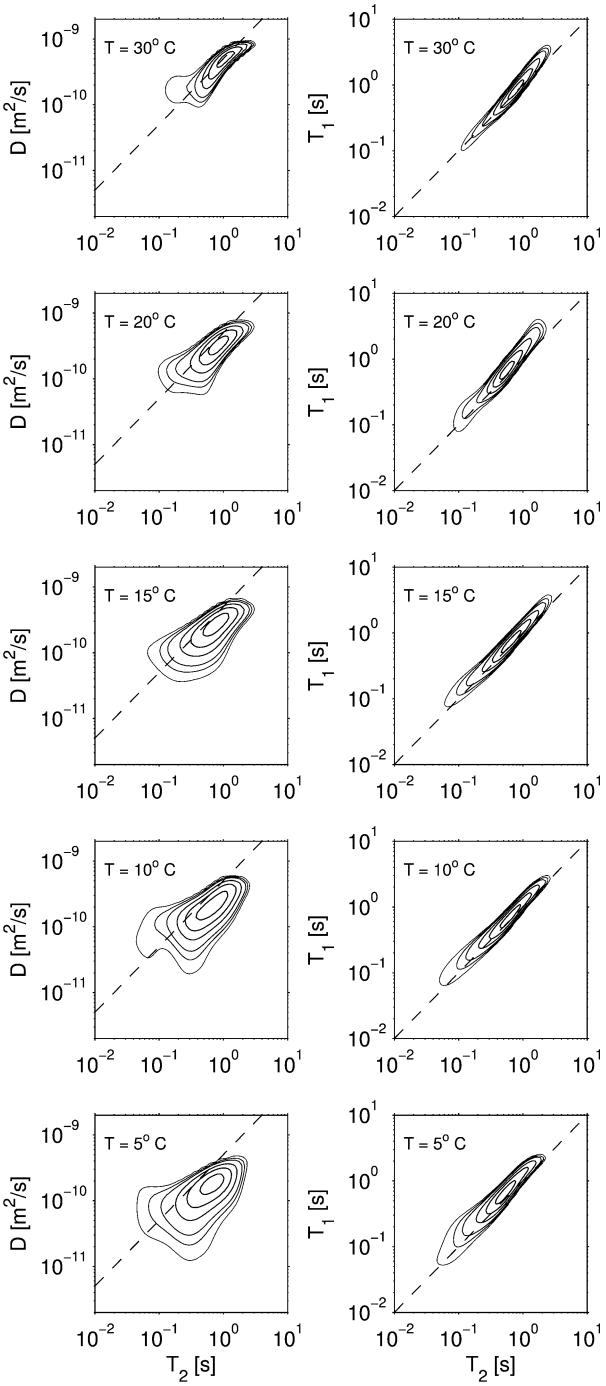

Figure 8. Diffusion−relaxation (left) and T_1-T_2 (right) distribution functions of a waxy oil (#1) at temperatures between 30 and 5 °C. As the temperatures is decreased from 30 °C, paraffins condense out and a gel is formed. This leads to a much larger decrease in the diffusion coefficient than relaxation time.

It is known that the rigid network can be formed by a small weight fraction of the sample; typical values of 4% were reported in ref 30. The relaxation times for the solid phase is very short and is not detected in our experiments. The presence of the gel network impedes the diffusion of the fluid molecules and leads to the lowering of the measured diffusion coefficients. However, the solid phase does not affect the relaxation of the liquid fraction significantly. We find that the T_1/T_2 ratio stays close to 1 over the whole temperature range studied. As the temperature is lowered, two opposing effects influence the relaxation times. A temperature decrease increases the internal viscosity, which lowers the relaxation times (see Figure 7). At

the same time, the composition of the liquid component changes, as long-chain molecules preferentially condense out at lower temperature.[31] This change of composition tends to lower the intrinsic viscosity and increase the relaxation times and counteracts the general temperature effect.

V. Discussion

A. Oils without Asphaltenes. For oils without asphaltenes (class I and II), the T_1-T_2 distribution functions show that $T_1 = T_2$ within experimental error over the entire range of relaxation times (after compensating for the diffusion induced artifact at long relaxation times). This implies that the spin dynamics is in the extreme motional averaging regime; i.e., all relevant motion is much faster than the Larmor frequency. There are no large, slowly tumbling aggregates present in these fluids.

For oils in the extreme motional averaging regime, we expect that the scaling laws for mixtures of linear alkanes discussed by Freed et al.[3,4] should be applicable. In this model the diffusion coefficient D_i of a component of chain length N_i in the mixture follows a power-law dependence on chain length:

$$D_i(N_i) = D(\bar{N})\left(\frac{N_i}{\bar{N}}\right)^{-\nu} \tag{5}$$

The exponent ν is temperature independent and was found to be $\nu = 0.7$ for a mixture of linear alkanes[3] and reflects the relationship between radius of gyration and chain length. The only temperature-dependent term is the prefactor $D(\bar{N})$, which is an overall property of the fluid mixture.

In an extension of the analysis to relaxation, Freed[4] showed that the relationship between relaxation times of the components in a mixture of linear alkanes and their chain lengths is given by an expression similar to eq 5. The theoretical analysis of relaxation is more complicated than the problem of diffusion because proton relaxation is affected both by internal motion and by rotational reorientation of the molecules, whereas translation diffusion only depends on the motion of the center of mass of each molecule. Nevertheless, Freed found that for mixtures of alkanes, the chain length dependence of the relaxation time of a component can still be approximated by a power law:

$$T_{2,i}(N_i) = T_2(\bar{N})\left(\frac{N_i}{\bar{N}}\right)^{-\kappa} \tag{6}$$

The exponent κ, determined by fitting experimental data of alkane mixtures to eq 6, was found to be $\kappa = 1.24 \pm 0.04$.[4] It is expected to be independent of temperature. The temperature dependence of the relaxation times is therefore determined by the temperature dependence of $T_2(\bar{N})$, an overall property of the fluid.

We can combine the two theoretical expressions for relaxation and diffusion, eqs 5 and 6, to obtain

$$\frac{D_i}{D(\bar{N})} = \left(\frac{T_{2,i}}{T_2(\bar{N})}\right)^{\nu/\kappa} \tag{7}$$

This equation has the same form as our phenomenological ansatz of eq 3.[25] We can now relate the exponent ζ to the exponents ν and κ:

$$\zeta = \nu/\kappa \tag{8}$$

For mixtures of alkanes, the expected value for the exponent ζ is therefore $\zeta = 0.56 \pm 0.02$. The experimental values for ζ are listed in Table 2 and are all within a factor of 1.5 of the value derived for alkane mixtures. Somewhat surprisingly, the saturate rich oils (class I) have exponents that are larger than the expected value for alkane mixtures, and the exponents for the aromatic rich oils (class II) are remarkably close to the theoretical alkane value.

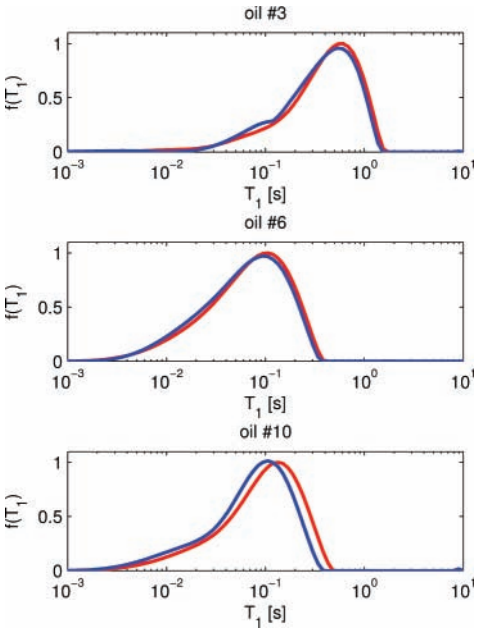

Figure 9. T_1 relaxation distribution functions for 3 oils at two different Larmor frequencies, 1.76 MHz (blue) and 5.03 MHz (red), for three oils with different composition. The top panel shows results for a saturate rich oil (#3), the middle panel for an oil rich in aromatics (#6), and the bottom panel for an oil with asphaltene (#10). Relaxation for oil #10 becomes faster at the lower Larmor frequency, confirming that asphaltene molecules lead to slow motion and the dynamics is not completely in the motional averaging regime anymore.

The composition of oils can be very complex. Even in oils with a large fraction of saturate molecules, linear *n*-alkanes are generally only a small component of these samples. Other saturate molecules such as branched and cyclic alkanes modify the relationship between carbon number and diffusion.[32] The systematic differences in the exponents ζ indicate that the relaxation times and diffusion coefficients not only are a function of the size of the molecules but also have a second-order dependence on the shape or chemical nature of the molecule. It is this sensitivity that makes these NMR measurements useful fingerprints of the oils. At the same time, it is remarkable to note that all crude oils without asphaltene are still well described by the relationship of the form of eq 7, which was initially derived for mixtures of alkanes.

B. Oils with Significant Asphaltene Content. ***1. Relaxation Measurements.*** In oils with significant amounts of asphaltenes, the longitudinal relaxation time T_1 is consistently longer than the transverse relaxation time T_2 for each component. This implies that the dynamics of these fluids are not in the motional averaging regime anymore. The motion has a component with a characteristic frequency that is comparable or smaller than the Larmor frequency. It is natural to associate this slow motion with the presence of large asphaltene aggregates.

For systems outside the motional averaging regime, the measured T_1 times are expected to be dependent on the Larmor frequency. In Figure 9 we compare the T_1 distributions at 5.03 MHz with those measured at 1.76 MHz, a reduction of about a factor of 3. For the oils without asphaltene (#3 and #6), the T_1 distributions for the two Larmor frequencies essentially overlay,

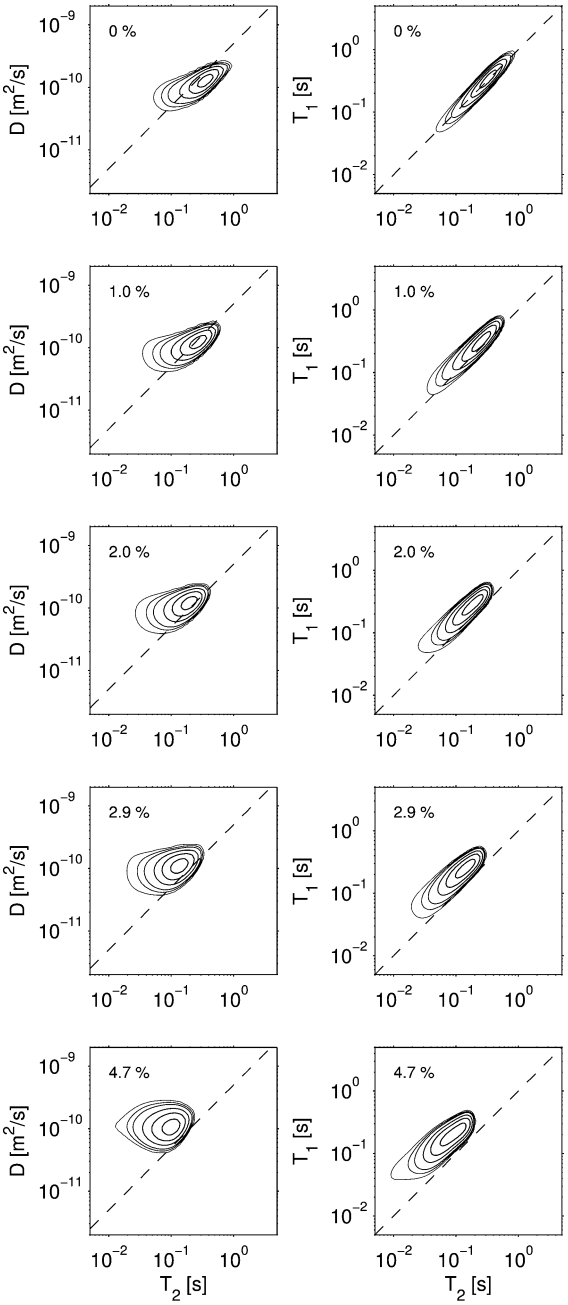

Figure 10. Diffusion$-T_2$ distributions functions (left) and T_1-T_2 distribution functions (right) for oil #8 doped with different amounts of asphaltene, as indicated in the figures. The dashed lines on the left are the alkane lines, and the dashed lines on the right indicate $T_1 = T_2$. As the asphaltene content is increased, the relaxation times systematically decrease and the main contributions in the $D-T_2$ distribution functions move away from the alkane line. Asphaltenes have a larger impact on T_2 than on T_1 relaxation: the contributions of the T_1-T_2 distribution functions move away from the T_1-T_2 correlation line with increasing asphaltene content.

further confirming that the dynamics is in the motional averaging regime. In contrast, the T_1 distributions for the oil with asphaltene (#10) are shifted and show a distinct frequency dependence.

Asphaltenes are generally the largest molecules in crude oil. These molecules easily aggregate and form large conglomerates that can reach macroscopic size.[14] The presence of such aggregates naturally leads to slow motion and explains the general features described.

However, some features of the data for oils with asphaltene in Figures 5 and 9 are rather remarkable and require further

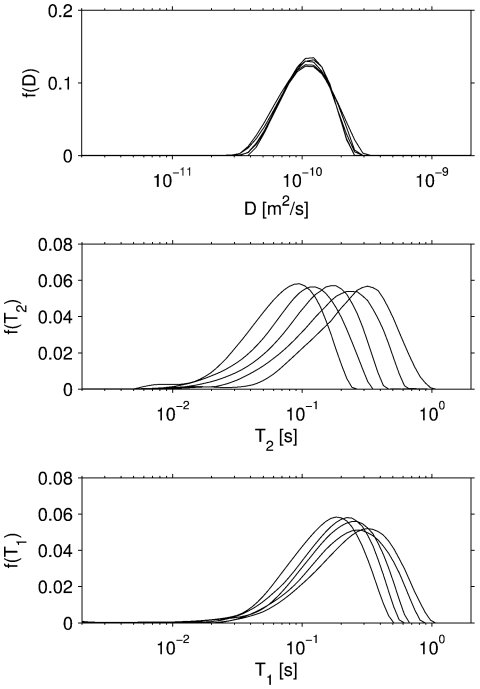

Figure 11. Projections of the two-dimensional distribution functions shown in Figure 10 for oil #8 with different asphaltene concentrations. In the top panel, the diffusion distribution function $f(D)$ obtained from the diffusion$-T_2$ distribution function are shown, whereas in the middle and lower panel, we show the T_2 and T_1 distribution functions, respectively, obtained from the measured T_1-T_2 distribution functions. The diffusion distributions $f(D)$ are essentially identical for all asphaltene concentrations. Increasing the asphaltene concentration shifts the T_2 distribution functions without distorting the shape significantly. The T_1 distributions are also shifted by asphaltene, but by a significantly smaller degree than for T_2.

discussion. In particular, Figure 5 shows that the presence of asphaltene increases the T_1/T_2 ratio for all components by about the same factor. One might have expected that the signal of asphaltene molecules appears at short relaxation times and that only this contribution displays an enhanced T_1/T_2 ratio. Similarly, in the bottom panel of Figure 9, all T_1 components are affected by the change of Larmor frequency, not only the fast relaxing components. This implies that the asphaltene molecules affect the dynamics of all oil molecules. In fact, the majority of the protons on the asphaltene are not detected directly with our experimental setup, as their intrinsic relaxation time is too short.[33] Instead, the asphaltene aggregates are detected indirectly by their effect on the relaxation properties of the other oil molecules. A more detailed analysis of this effect will be presented elsewhere.

2. Diffusion−Relaxation Measurements. For oils with asphaltene, the main contributions of $f(D,T_2)$ are located well away from the alkane line. In principle, this shift could be caused by diffusion that is anomalously high, or by relaxation that is anomalously fast. An increased relaxation rate is much more plausible, and has in fact already been reported for asphaltene in simple solvents.[34,35] Results presented in Figure 10 show that asphaltene molecules also act as relaxation contrast agents in these more complex samples. In these experiments, asphaltene was systematically added to oil #8. As shown on the left-hand side of Figure 10, the addition of asphaltene leads to a characteristic shortening of the relaxation times of all components. Furthermore, the ratio T_1/T_2 increases gradually with asphaltene concentration. As asphaltene is added, the main feature in the T_1-T_2 distribution function transforms from a narrow ridge along the $T_1/T_2 = 1$ line to a somewhat broader

TABLE 3: Overview of Relationships between Fluid Composition and Measured NMR Properties $f(D,T_2)$ and $f(T_1,T_2)$

	fluid properties	NMR properties
class I "saturate rich"	high in saturates no asphaltene monotonic GC above C10	$\zeta \sim 0.7-0.85$ $D - T_2$ close to alkane line $T_1 = T_2$
class II "aromatic rich"	high in aromatics no asphaltene nonmonotonic GC above C10	$\zeta \sim 0.5$ $D - T_2$ close to alkane line $T_1 = T_2$
class III "asphaltene"	significant amount of asphaltene (>1%)	$T_1 > T_2$ $D - T_2$ above alkane line T_1 dependence on f_{Larmor}

ridge at a higher T_1/T_2 ratio. The features of the two-dimensional distribution functions continuously change from those associated with class II to those of class III.

It is interesting to compare the effect of asphaltene to that of oxygen and other paramagnetic contrast agents widely used in medical imaging.[36] To first order, a contract agent increases the relaxation rate of the oil component i as follows:

$$\frac{1}{T_{2,i}} = (1-\epsilon)\frac{1}{T_{2,i}}\bigg|_{\text{oil}} + \epsilon\,\frac{1}{T_{2,i}}\bigg|_{\text{asph}} \tag{9}$$

Here $T_{2,i}|_{\text{oil}}$ is the relaxation time of the oil without asphaltene and ϵ is the fraction of time that the oil molecule is in the vicinity of the asphaltene aggregate experiencing an extra relaxation rate $1/T_{2,i}|_{\text{asph}}$. The effect of oxygen on the relaxation of crude oil were studied in[16] and could be accurately described with an expression equivalent to eq 9, using values for ϵ and the extra relaxation rate that were uniform for all components within a given oil. The remarkable feature for asphaltene is that the asphaltene induced relaxation rates $\epsilon\ 1/T_{2,i}|_{\text{asph}}$ are not identical for all components of an oil but depend on the relaxation rate of the component. This effect is particularly evident in Figure 11 that displays the one-dimensional distribution functions for diffusion, T_2, and T_1, obtained by projection of the data shown in Figure 10 for the five different asphaltene concentrations. In this system, increasing the asphaltene concentration shifts the T_1 and T_2 distribution functions without distorting the shape significantly, whereas it has very little effect on the diffusion distribution, i.e., $f(D,T_2) \rightarrow f(D,T_2/\lambda_{T_2})$ and $f(T_1,T_2) \rightarrow f(T_1/\lambda_{T_1},T_2/\lambda_{T_2})$.

We expect that the effect of asphaltene on the other oil molecules is a strong function of its aggregation state. Unlike most other techniques that are used to study the aggregation state of asphaltene, the current technique is not limited to model systems but can be used in crude oil. A more detailed analysis and theoretical description will be presented elsewhere.

VI. Conclusion

We have demonstrated that two-dimensional diffusion$-T_2$ and T_1-T_2 distribution functions can be used to characterize complex fluids. In the hydrocarbon oils studied here, we were able to correlate specific features in the distribution functions with general properties of the chemical composition. A summary of the observed effects are listed in Table 3. These relationships hold over the whole temperature range studied, i.e., between 10 and 50 °C, unless a waxing transition occurs.

In addition to the general information on chemical composition, the power-law relationships developed by Freed et al.[3,4] for alkane mixtures can be used to extract an approximate distribution of chain lengths from the measured distributions of relaxation times or diffusion coefficients. The T_1-T_2 distribution functions measured in our experiments are particularly sensitive to slow motion associated with a characteristic frequency of a few MHz or below. For this reason, it is well suited to study the process of the aggregation of asphaltene or other large molecules. We have shown here that such asphaltene aggregates act as relaxation contrast agents, without affecting the diffusion properties of the other oil molecules significantly.

The present study focused on hydrocarbon oil. We expect that this general approach should be useful to the study of a much wider class of fluids with different chemical composition. To first order, the diffusion coefficient and the low-field relaxation time of a component is determined by its molecular size and the internal viscosity of the mixture.[3,4] However, the specific shapes, chemical properties and interactions of the molecules will modify the relationships. In general, these effects will not be the same for diffusion and relaxation. As a consequence, the simultaneous measurement of diffusion and relaxation with the distribution functions encodes this chemical information.

This approach based on distribution functions is well suited for complex fluids with a wide range of components. It is also useful for the study of multiphase and other structured fluids. An example of an emulsion has been reported in ref 37 for the case of a dairy products. In that application, the measured mean squared displacement is determined by the bubble size rather than the molecular diffusion coefficient. This leads to an effective diffusion coefficient that is independent of relaxation time.

Finally, it is worthwhile to emphasize that these techniques are noninvasive and can be performed as ex-situ measurements.[38] These NMR measurements can be performed in inhomogeneous magnetic fields of relatively low field strength. The required instrumentation for this approach is therefore much less demanding than for conventional NMR spectroscopy.

Acknowledgment. We thank Denise Freed for enlightening discussions on the theory of diffusion and relaxation in mixtures, Yi-Qiao Song and Lauren Burcaw for sharing diffusion measurements on waxy oils, and Abdel Kharrat for preparing samples with different asphaltene concentration, performing oil analysis, and for numerous discussions on the chemical properties of crude oils.

References and Notes

(1) Grob, R. L., Barry, E. F., Eds. *Modern Practice of Gas Chromatography*, 4th ed.; Wiley-Interscience: New York, 2004.

(2) Marshall, A. G. Milestones in fourier transform ion cyclotron resonance mass spectrometry technique development. *Int. J. Mass Spectrom.* **2000**, *200*, 331−356.

(3) Freed, D. E.; Burcaw, L.; Song, Y.-Q. Scaling laws for diffusion coefficients in mixtures of alkanes. *Phys. Rev. Lett.* **2005**, *94*, 067602.

(4) Freed, D. E. Dependence on chain length of NMR relaxation times in mixtures of alkanes. *J. Chem. Phys.* **2007**, *126*, 174502.

(5) Pedersen, K. S.; Christensen, P. L. *Phase Behavior of Petroleum Reservoir Fluids*; Taylor & Francis: London, 2007.

(6) Ernst, R. R.; Bodenhausen, G.; Wokaun, A. *Principles of Nuclear Magnetic Resonance in One and Two Dimensions*; Clarendon Press: Oxford, 1987.

(7) Hürlimann, M. D.; Venkataramanan, L. Quantitative measurement of two dimensional distribution functions of diffusion and relaxation in grossly inhomogeneous fields. *J. Magn. Reson.* **2002**, *157*, 31−42.

(8) Song, Y.-Q.; Venkatarmanan, L.; Hürlimann, M. D.; Flaum, M.; Frulla, P.; Straley, C. Correlation spectra obtained using a fast two-dimensional Laplace inversion. *J. Magn. Reson.* **2002**, *154*, 261−268.

(9) Bloembergen, N.; Purcell, E. M.; Pound, R. V. Relaxation effects in nuclear magnetic resonance absorption. *Phys. Rev.* **1948**, *73*, 679−712.

(10) Kowalewski, J.; Mäler, L. *Nuclear Spin Relaxation in Liquids: Theory, Experiments, and Applications*; Taylor & Francis: New York, London, 2006.

(11) Kimmich, R.; Fatkullin, N. Polymer chain dynamics and NMR. *Adv. Polym. Sci.* **2004**, *170*, 1−113.

(12) Tissot, B. P.; Welte, D. H. *Petroleum Formation and Occurrence*; Springer: Berlin, 1984.

(13) McCain, W. D., Jr. *The properties of petroleum fluids*; PennWell Publishing Co.: Tulsa, OK, 1990.

(14) Mullins, O. C., Sheu, E. Y., Hammami, A., Marshall, A., Eds. *Asphaltenes, Heavy Oils and Petroleomics*; Springer: Berlin, 2006.

(15) Hürlimann, M. D.; Flaum, M.; Venkataramanan, L.; Flaum, C.; Freedman, R.; Hirasaki, G. J. Diffusion-relaxation distribution functions of sedimentary rocks in different saturation states. *Magn. Reson. Imaging* **2003**, *21*, 305−310.

(16) Mutina, A. R.; Hürlimann, M. D. Effect of oxygen on the NMR relaxation properties of crude oils. *Appl. Magn. Reson.* **2005**, *29*, 503−514.

(17) Suatoni, J. C.; Swab, R. E. Rapid hydrocarbon group-type analysis by high performance liquid chromatography. *J. Chromatogr. Sci.* **1975**, *13*, 361−366.

(18) Fan, T.; Buckley, J. S. Rapid and accurate SARA analysis of medium gravity crude oils. *Energy Fuels* **2002**, *16*, 1571−1575.

(19) Kharrat, A. Personal communication, 2006.

(20) Hürlimann, M. D.; Venkataramanan, L.; Flaum, C. The diffusion-spin relaxation time distribution function as an experimental probe to characterize fluid mixtures in porous media. *J. Chem. Phys.* **2002**, *117*, 10223−10232.

(21) Venkataramanan, L.; Song, Y.-Q.; Hürlimann, M. D. Solving Fredholm integrals of the first kind with tensor product structure in 2 and 2.5 dimensions. *IEEE Trans. Signal Processing* **2002**, *50*, 1017−1026.

(22) Carr, H. Y.; Purcell, E. M. Effects of diffusion on free precession in nuclear magnetic resonance experiments. *Phys. Rev.* **1954**, *94*, 630−638.

(23) Kimmich, R.; Unrath, W.; Schnur, G.; Rommel, E. measurement of small self-diffusion coefficients in the fringe field of superconducting magnets. *J. Magn. Reson.* **1991**, *91*, 136−140.

(24) Lo, S.-W.; Hirasaki, G. J.; House, W. V.; Kobayashi, R. Mixing rules and correlations of NMR relaxation time with viscosity, diffusivity, and gas/oil ratio of methane/hydrocarbon mixtures. *SPEJ* **2002**, *7*, 24−34.

(25) Hürlimann, M. D. Diffusion-relaxation distribution functions of miscible fluids measured in grossly inhomogeneous fields. *Appl. Magn. Reson.* **2004**, *25*, 651−660.

(26) Hürlimann, M. D. Diffusion and relaxation effects in general stray field NMR experiments. *J. Magn. Reson.* **2001**, *148*, 367−378.

(27) Straley, C. Reassessment of correlations between viscosity and NMR measurements. *Trans. SPWLA 47rd Annual Logging Symposium* **2006**, Paper AA.

(28) Abdallah, D. J.; Weiss, R. G. n-alkanes gel n-alkanes (and many other organic liquids). *Langmuir* **2000**, *16*, 352−355.

(29) Abdallah, D. J.; Sirchio, S. A.; Weiss, R. G. Hexatriacontane organogels. the first determination of the conformation and molecular packing of a low-molecular-mass organogelator in its gelled state. *Langmuir* **2000**, *16*, 7558−7561.

(30) Pedersen, W. B.; Hansen, A. B.; Larsen, E.; Nielsen, A. B.; Rønningsen, H. P. Wax precipitation from North Sea crude oils. 2. Solid-phase content as function of temperature determined by pulsed NMR. *Energy Fuels* **1991**, *5*, 908−913.

(31) Singh, P.; Venkatesan, R.; Fogler, H. S.; Nagarajan, N. Formation and aging of incipient thin film of wax-oil gels. *AIChE J.* **2000**, *46*, 1059−1074.

(32) von Meerwall, E.; Ozisik, R.; Mattice, W. L.; Pfister, P. M. Self-diffusion of linear and cyclic alkanes, measured with pulsed-gradient spin-echo nuclear magnetic resonance. *J. Chem. Phys.* **2003**, *118*, 3867−3873.

(33) Lisitza, N. V.; Freed, D. E.; Sen, P. N.; Song, Y. Q. Self-assembly of asphaltenes: Enthalpy, entropy of depletion and dynamics at the crossover. To be published.

(34) Poindexter, E. Double resonance and proton relaxation in asphalt solutions. *J. Chem. Phys.* **1962**, *37*, *463*−468.

(35) Jestin, J.; Barré, L. Application of NMR solvent relaxation and SAXS to asphaltenes solutions characterization. *J. Disp. Sci. Technol.* **2004**, *25*, 341−347.

(36) Boxerman, J. L.; Hamberg, L. M.; Rosen, B. R.; Weisskoff, R. M. MR contrast due to intravascular magnetic susceptibility perturbations. *Magn. Reson. Med.* **1995**, *34*, 555−566.

(37) Hürlimann, M. D.; Burcaw, L.; Song, Y. Q. Quantitative characterization of food products by two-dimensional $D-T_2$ and T_1-T_2 distribution functions in a static gradient. *J. Colloid Interface Sci.* **2006**, *297*, 303−311.

(38) Hürlimann, M. D.; Venkataramanan, L.; Flaum, C.; Speier, P.; Karmonik, C.; Freedman, R.; Heaton, N. Diffusion-editing: New NMR measurement of saturation and pore geometry. *Trans. SPWLA 43rd Annu. Logging Symp., Oiso, Jpn.* 2002, Paper FFF.